Jurnal Rekayasa Mesin
p-ISSN: 1411-6863, e-ISSN: 2540-7678
Vol.21, No.1, April **2026**, p. 129-138

Impact of Endurance Testing on the Thermal Performance of a Retrofitted FDM 3D Printer

David Christanto[1], Laurentius Yudha Bramantyo[1], Bondan Wiratmoko Budi Santoso[2*], Alexander Ariantono Nugroho[1], Ign. R. Haryosuprobo[1] and Mardiatno[1]
[1]Program Studi Sarjana Terapan Teknologi Rekayasa Mekatronika, Politeknik ATMI Surakarta,
Jl. Mojo No.1, Karangasem, Kec. Laweyan, Kota Surakarta, Jawa Tengah 57145, Indonesia
[2] Program Studi Sarjana Terapan Perancangan Manufaktur, Politeknik ATMI Surakarta,
Jl. Mojo No.1, Karangasem, Kec. Laweyan, Kota Surakarta, Jawa Tengah 57145, Indonesia
*E-mail: bondanwiratmoko69@gmail.com

Submitted: 12-09-2025; Accepted: 24-04-2026; Published: 30-04-2026

Abstract

The reliability of retrofitted Fused Deposition Modeling (FDM) 3D printers is affected by thermal stability during long print cycles. This study evaluated the thermal performance of a retrofitted BFB 3D Touch Cartesian FDM printer equipped with dual extruders, automatic bed leveling, a BTT SKR v1.4 controller, and a 24 V/360 W power supply unit (PSU). An 80 × 80 × 80 mm calibration cube was printed for 5 h to impose a continuous thermal load. Surface temperatures of stepper drivers, stepper motors, mainboard, PSU, and heated bed were measured with a TR-10 thermal imager at 1 h intervals, while bed preheating was recorded for 7 min at P1-P4 and the bed center. The Y1 driver reached 68.7 °C at hour 3, the PSU reached 65.0 °C at hour 5, and the extruder motor reached 52.7 °C. The bed center reached 59.2 °C at minute 7, but the corner regions were lower and locally non-monotonic. These fluctuations are interpreted as effects of local heat-transfer non-uniformity and measurement instability rather than uniform bed cooling. This study shows that driver and PSU cooling, cable-size verification, repeated measurements, and bed insulation are required to improve retrofit-printer reliability in extended operation.

Keywords: *3D printer; endurance test; FDM; thermal behavior; thermal management*

Abstrak

Keandalan mesin Fused Deposition Modeling (FDM) hasil retrofit dipengaruhi oleh kestabilan termal selama pencetakan berdurasi panjang. Penelitian ini mengevaluasi kinerja termal mesin 3D printer FDM retrofit berbasis BFB 3D Touch Cartesian yang dilengkapi dual extruder, automatic bed leveling, kontroler BTT SKR v1.4, dan power supply unit (PSU) 24 V/360 W. Spesimen kubus kalibrasi 80 × 80 × 80 mm dicetak selama 5 jam sebagai beban termal kontinu. Suhu permukaan stepper driver, motor stepper, mainboard, PSU, dan heated bed diukur menggunakan thermal imager TR-10 pada interval 1 jam, sedangkan respons pemanasan bed direkam selama 7 menit pada P1-P4 dan titik tengah bed. Hasil penelitian menunjukkan bahwa driver Y1 mencapai 68,7 °C pada jam ke-3, PSU mencapai 65,0 °C pada jam ke-5, dan motor ekstruder mencapai 52,7 °C. Titik tengah bed mencapai 59,2 °C pada menit ke-7, tetapi daerah sudut lebih rendah dan tidak selalu meningkat secara monoton. Fluktuasi ini diinterpretasikan sebagai pengaruh ketidakseragaman perpindahan panas lokal dan ketidakstabilan pengukuran, bukan pendinginan merata pada bed. Penelitian ini menunjukkan bahwa pendinginan driver dan PSU, verifikasi ukuran kabel, pengulangan pengukuran, serta isolasi bed diperlukan untuk meningkatkan keandalan mesin retrofit pada operasi berdurasi panjang.

Kata kunci: 3D printer; FDM; manajemen termal; perilaku termal; uji endurance

1. Introduction

The growing adoption of additive manufacturing technologies, particularly Fused Deposition Modeling (FDM), has increased the demand for reliable, durable, and thermally stable 3D printing systems [1]. In an FDM machine, heat is generated not only at the hot end and heated bed, but also in the motor drivers, stepper motors, mainboard, power supply unit (PSU), and electrical connections during prolonged operation. Excessive or uneven heat accumulation can reduce print consistency, accelerate component aging, and increase the risk of maintenance problems [2].

Previous studies on FDM/FFF thermal behavior have mainly focused on material deposition, nozzle heat transfer, hot-end heat sinks, or the temperature history of printed parts [3-4]. Experimental data from polymer extrusion additive manufacturing indicate that the build platform and near-bed air temperature strongly affect filament-bed interaction,

cooling rate, and interlayer bonding [5; 13-14]. Reviews of in-process temperature monitoring also show that thermal history is directly related to interlayer adhesion and the quality of printed parts [15].

However, direct measurement of whole-machine thermal behavior during an endurance test is still limited, especially for retrofitted machines whose mechanical, electrical, and control systems differ from the original factory design. The present study addresses this gap by measuring the temperature distribution of critical machine components and the heated bed of a retrofitted BFB 3D Touch Cartesian printer during a 5-hour print test.

The objective of this study is to identify components that are susceptible to heat accumulation, compare local bed-temperature readings with the built-in bed sensor, and formulate practical recommendations for cooling, wiring, and bed insulation. The results are intended to support preventive maintenance and improve operational reliability when the machine is used for longer prints or higher-temperature filament applications [6].

2. Material and Method

2.1. Material and Instrument

2.1.1 Retrofitted FDM 3D Printer based on the BFB 3D Touch

The retrofitted printer used as the test object is shown in Figure 1. Figure 1(a) represents the original BFB 3D Touch model, Figure 1(b) shows the non-operational machine before retrofitting, and Figure 1(c) shows the machine after mechanical and electronic modifications.

(a) (b) (c)

Figure 1. Condition of BFB 3D Touch 3D Printer, (a) initial model, (b) before retrofitting and (c) after retrofitting

The primary equipment was a retrofitted FDM 3D printer based on the BFB 3D Touch model, which uses a Cartesian motion system. The previously non-operational machine was restored through mechanical and electronic retrofitting. The retrofit included dual extruders and automatic bed leveling to improve print consistency [7]. All drivers and stepper motors were kept in the same configuration during the test; therefore, this study evaluates the baseline thermal performance of the current retrofit configuration rather than comparing different motor-driver variants.

- Mainboard: BTT SKR v1.4
- Display: BTT TFT43
- Hotend: Multi color nozzle with 2-in-1-out configuration
- Auto-leveling: BLTouch via Raspberry Pi & Arduino
- Bed size: 215 mm x 215 mm x 185 mm
- Power: 24V 360W PSU

2.1.2 Thermal Imager TR-10

The TR-10 thermal imager (Figure 2) was used to measure the surface temperature of the heated bed, stepper drivers, stepper motors, mainboard, PSU, and supporting structures. Its imaging capability allowed the same region of interest (ROI) to be observed repeatedly during the endurance test [8].

Figure 2. Thermal Imager TR-10

- 192 x 192 IR Resolution & 25 Hz Frame Rate
- 2.8" LCD Display with 240 x 240 Resolution
- 50° Wide Angle Lens
- Precise Readings with ±2% Accuracy
- Measurable Distance Range : 0.3 m to 3 m (1 ft to 10 ft)
- Spectral Range : 8 µm to 14 µm
- Temperature Range : –20°C to 550°C (–4°F to 1022°F)

2.2. Experimental Procedure

The endurance specimen and printing condition are shown in Figure 3. The specimen was used to impose a continuous thermal load on the retrofitted printer during the observation period.

Figure 3. Printing specimen of 80 × 80 × 80 mm calibration cube for 5-hour endurance testing

The experimental method was designed to evaluate the thermal behavior and heat dissipation characteristics of the retrofitted machine under prolonged operation. The printer continuously fabricated a non-standard 80 × 80 × 80 mm

calibration cube for 5 h at the default print speed. This specimen was selected instead of the commonly used 20 × 20 × 20 mm calibration cube because the smaller specimen requires a shorter printing time and does not provide a sufficient endurance load. The cube therefore served as a controlled thermal-loading specimen, not as a complete representation of all possible product geometries [9].

Component temperatures were measured at Hour 0, Hour 1, Hour 2, Hour 3, Hour 4, and Hour 5. The observed components included the stepper drivers, stepper motors, mainboard, PSU, and heated bed. The orange circles in Figure 4 indicate thermal ROIs. Each component ROI was selected as a nominal 10 mm diameter circular area located at the center of the target component surface. For the bed preheating test, five ROIs were used: P1, P2, P3, and P4 at the four corner regions of the 215 × 215 mm bed, and one ROI at the bed center. The corner ROIs were positioned approximately 20 mm from the nearest bed edges, while the center ROI was located approximately 107.5 mm from both bed edges, as illustrated in Figure 5.

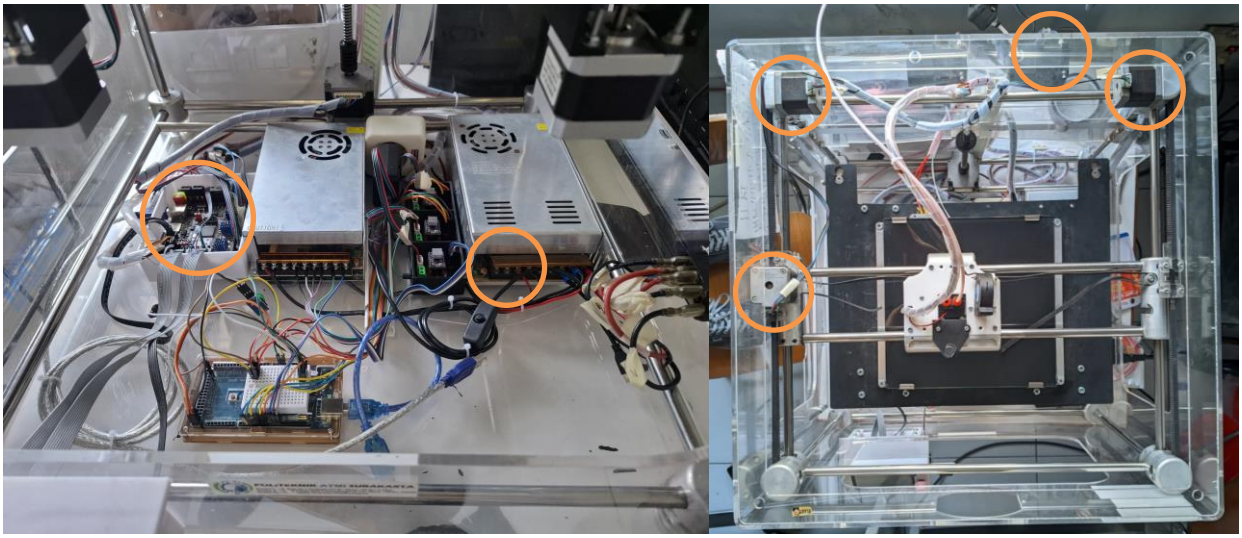

(a) (b)

Figure 4. Thermal data acquisition ROIs: (a) mainboard and PSU area and (b) stepper-motor and cable area; orange circles indicate nominal 10 mm diameter measurement regions

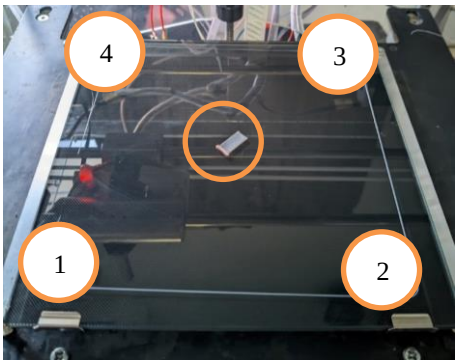

Figure 5. Bed thermal data acquisition points P1-P4 and bed center on the 215 × 215 mm bed

The recorded data from the thermal imager were compared with the built-in bed temperature sensor readings to analyze thermal uniformity and possible sensor deviation. Heat propagation toward the bed frame and mounting bolts was also observed to indicate heat dissipation through the supporting structure [10]. Because the available dataset was obtained

from a single endurance run, the analysis is descriptive. Repeating the test at least three times with a fixed camera mount, constant emissivity setting, and identical ROI positions is recommended to obtain average values, standard deviations, and error bars.

The simplified flowchart in Figure 6 summarizes the sequence of machine preparation, endurance printing, thermal data acquisition, and comparison between thermal-imager and built-in sensor readings.

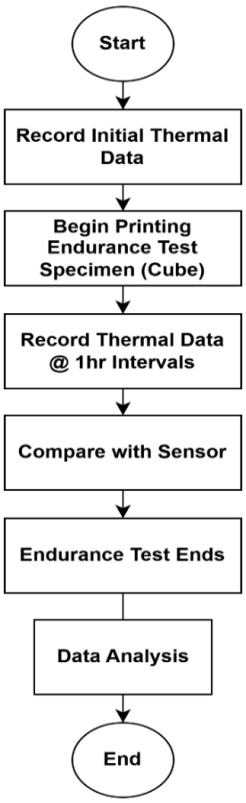

Figure 6. Experimental procedure flowchart

3. Results and Discussion

3.1. Component Thermal Analysis

The endurance-test data were analyzed to identify components with the highest thermal load and to evaluate whether the temperature trend stabilized, increased, or decreased during the final hour of operation. Table 1 summarizes the hourly temperature response of the motor drivers, stepper motors, mainboard, and PSU during the five-hour endurance test.

Table 1. Component Temperature by Hour on the Endurance Test

Components	Component Temperature (°C)					
	Hour 0	Hour 1	Hour 2	Hour 3	Hour 4	Hour 5
Driver Motor X	35.8	61.3	61.6	61.8	60.6	45.7
Driver Motor Y1	37.2	66.9	67.3	68.7	67.9	48.2
Driver Motor Y2	35.6	63.1	57.2	62.4	61.9	44.7

Driver Motor Z	39.5	57.9	58.0	57.7	55.9	45.9
Driver Motor E	34.6	38.0	38.0	38.2	39.1	38.8
Stepper Motor X	28.2	42.9	43.1	42.5	41.4	41.2
Stepper Motor Y1	27.7	29.7	30.1	30.3	29.2	29.7
Stepper Motor Y2	27.9	29.8	30.3	30.3	29.4	29.5
Stepper Motor Z	28.9	28.9	28.5	29.5	27.9	27.3
Stepper Motor E	27.6	49.3	50.8	52.7	50.5	46.5
Mainboard BTT SKR V1.4	41.9	49.6	49.0	49.6	49.4	45.4
PSU 24V	59.4	56.7	48.4	55.3	57.3	65.0

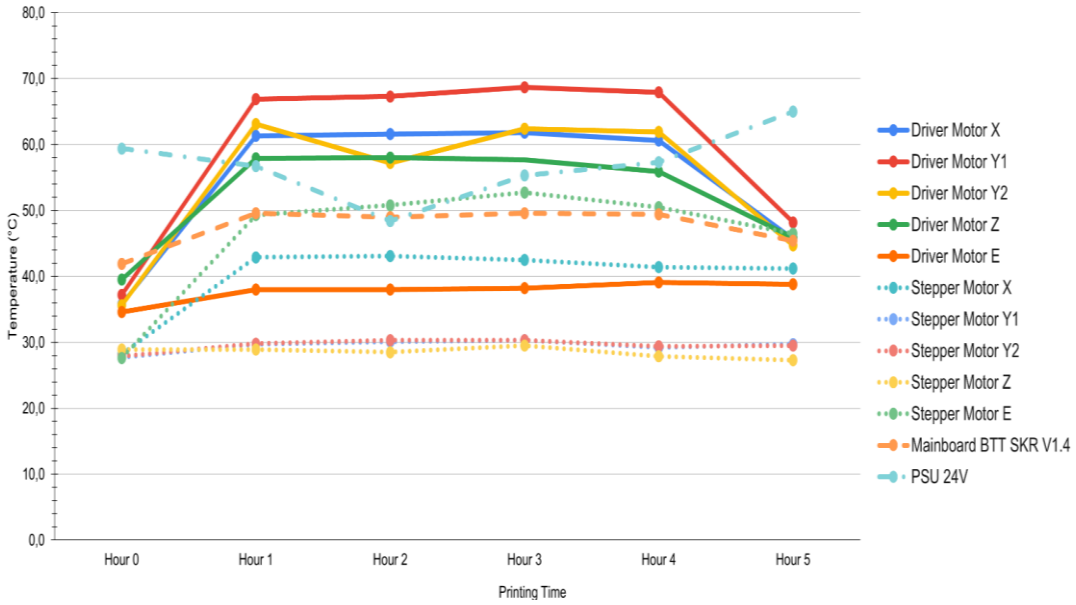

Figure 7. Graph of components temperature during 5-hour endurance test

Figure 7 visualizes the data in Table 1 and shows that the motor drivers reached high temperatures more rapidly than most stepper motors. Driver Y1 recorded the highest value, 68.7 °C at Hour 3, while Driver X and Driver Y2 remained mostly above 60 °C between Hour 1 and Hour 4. In contrast, the E driver remained near 38-39 °C, although the extruder motor increased to 52.7 °C at Hour 3. This difference indicates that motor-body heating and driver-board heating are not identical thermal phenomena; they are affected by current setting, duty cycle, airflow exposure, heat-sink contact, and the physical location of the component.

- Highest extruder motor temperature: 52.7 °C at Hour 3
- Highest driver temperature: 68.7 °C at Hour 3 on Driver Y1

The temperature decrease of several motor drivers at Hour 5, as shown in Figure 7, is likely related to a reduction in motion duty cycle when the print approached completion or entered a lower-load interval. Stepper motors and drivers convert electrical losses into heat based on current, holding torque, and motion demand. Therefore, a lower movement load can reduce driver temperature even though the machine is still powered. However, the PSU reached 65.0 °C at Hour

5, which suggests heat accumulation in the power-supply area, insufficient ventilation, contact resistance at power terminals, or a delayed response of the PSU casing temperature. Previous studies of FFF heat transfer confirm that temperature history is strongly influenced by process conditions, local air temperature, build-plate environment, and measurement location [14-18].

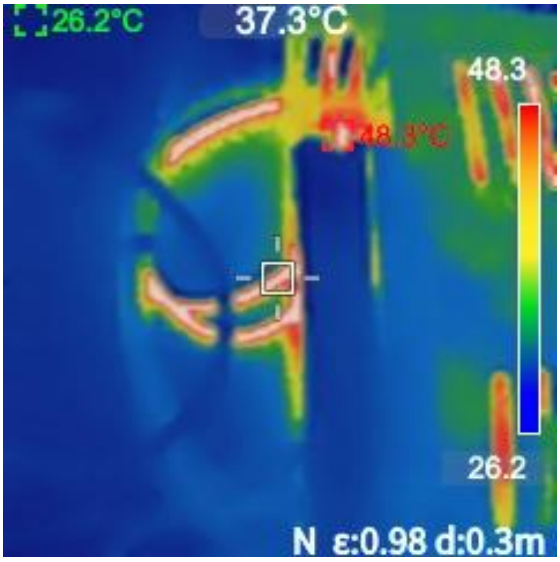

Figure 8. Thermal image of the 24 V power cable from the PSU

The thermal concentration shown in Figure 8 should be interpreted as a local hot spot rather than direct evidence of combustion. Possible causes include an insufficient conductor cross-sectional area, terminal contact resistance, cable routing near heat sources, or weak airflow around the PSU. Before additional electrical features are installed, the cable gauge, terminal crimp quality, and PSU cooling path should be checked against the maximum current requirement. Additional heat sinks or fans in the driver area and improved PSU ventilation are recommended to reduce thermal stress and support long-term machine reliability.

3.2. Bed Temperature Distribution

During the bed preheating test, the surface-temperature response was measured at P1, P2, P3, P4, and the bed center, as defined in Figure 5. Table 2 presents the temperature readings during the 7-minute preheating phase for the target bed temperature of 60 ± 2 °C.

Table 2. Thermal Dissipation of Bed Pre-Heating Phase

Position	Component Temperature (°C)							
	Minute 0	**Minute 1**	**Minute 2**	**Minute 3**	**Minute 4**	**Minute 5**	**Minute 6**	**Minute 7**
P1	27.60	30.00	35.80	36.40	35.10	36.20	28.00	37.80
P2	27.70	30.40	36.50	38.00	44.00	42.60	28.20	47.50
P3	28.00	33.60	38.00	41.00	36.10	42.60	38.50	33.20
P4	27.80	32.80	35.40	31.70	42.80	38.30	36.60	38.00
BED	27.70	34.90	40.50	45.50	50.60	53.20	58.10	59.20

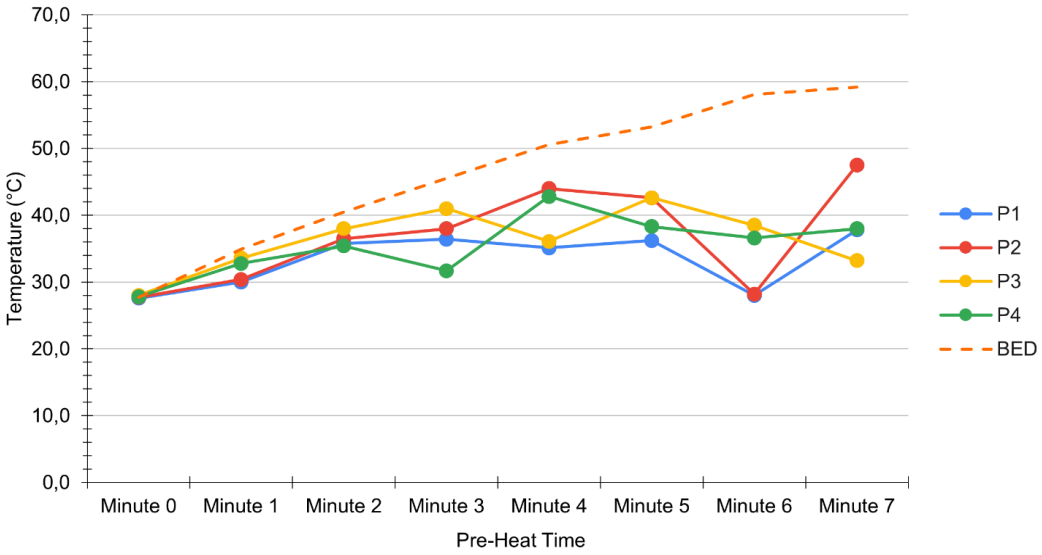

Figure 9. Graph of bed preheat temperature imaging

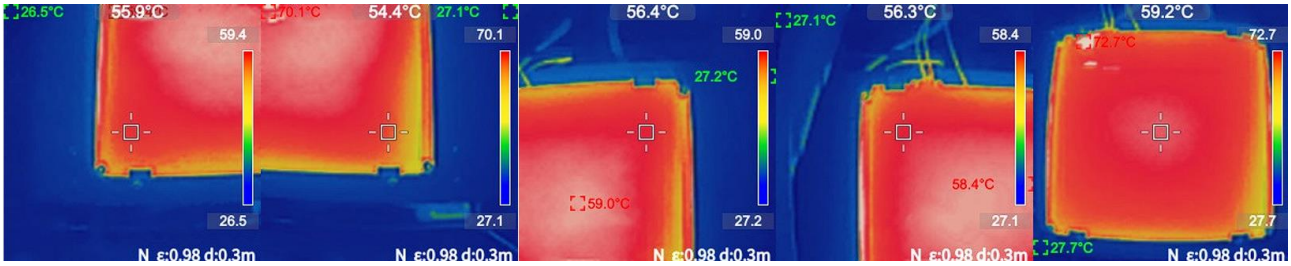

Figure 10. Result of 7-minute bed preheating

Table 2 and Figure 9 show two important trends. First, the bed center increased monotonically from 27.7 °C to 59.2 °C, indicating that the heater and built-in control system raised the central bed temperature toward the target range. Second, the four corner ROIs did not increase uniformly. At Minute 7, the corner readings ranged from 33.2 °C at P3 to 47.5 °C at P2, while the bed center reached 59.2 °C. This condition indicates that the corner regions lagged behind the center during preheating. Similar build-plate studies have reported that heat transfer near the bed, local convection, and in-plane temperature fields strongly influence filament-bed thermal interaction [5; 13-14].

The sharp local decreases at P1 and P2 after Minute 6, at P3 during Minutes 4 and 6-7, and at P4 after Minute 4 are not likely to represent true uniform cooling of the glass bed, because the thermal mass of the bed cannot physically cool by more than 10 °C within one minute while the bed center continues to increase. These non-monotonic values are more reasonably attributed to local measurement instability, including ROI shift, reflected radiation from the glass surface, emissivity differences, measurement angle, or accidental measurement of edge/bolt regions rather than the same bed surface. Therefore, the bed data should be interpreted as local surface readings from a single trial. Reproducibility should be verified through repeated experiments using a fixed camera position, emissivity correction tape, and identical ROI definitions.

Figure 10 supports the interpretation that the central zone and heater-contact region were warmer than the bed edges. The non-uniformity may originate from the glass bed material, non-uniform heater contact pressure, heat losses to the open air, and the absence of sufficient insulation below the bed. For printing more complex shapes, the thermal response

may differ because travel path, infill density, print time, retraction frequency, and layer cooling vary with geometry. Consequently, the present results should be treated as a baseline assessment for the 80 × 80 × 80 mm cube configuration, not as a universal endurance conclusion for all product shapes [16-17].

4. Conclusion

The 5-hour single-run endurance test of the retrofitted BFB 3D Touch FDM printer provided a baseline thermal assessment for the 80 × 80 × 80 mm cube loading condition. The component-temperature data showed that Driver Y1 was the most critical driver, reaching 68.7 °C at Hour 3, while the PSU reached 65.0 °C at Hour 5. The extruder motor reached 52.7 °C, indicating sustained motor heating during material extrusion.

- The bed preheating data showed non-uniform center-to-corner thermal behavior. The center reached 59.2 °C at Minute 7, whereas the corner ROIs remained lower and showed several non-monotonic readings. These fluctuations indicate the need for improved bed-insulation design and more repeatable thermal-imaging procedures.
- The hour-5 decrease of several motor drivers is likely related to reduced motion load near print completion, while the late PSU peak indicates that the power-supply cooling path requires attention.

Future work should repeat the endurance test at least three times, report average temperatures with error bars, and evaluate the printed product through dimensional accuracy, surface quality, and mechanical or functional tests. Additional studies with more complex geometries are also required before the endurance performance can be generalized beyond the current cube specimen. Practical improvements include redesigning airflow paths, adding active cooling to driver and motor sections, verifying cable gauge and terminal resistance, and applying insulation under the heated bed.

Acknowledgement

The authors express their gratitude to the Program Studi Teknologi Rekayasa Mekatronika, Fakultas Teknik, Politeknik ATMI Surakarta, for providing facilities and technical support during the retrofitting and endurance testing activities.

References

[1] Zagidullin, R., Mitroshkina, T., and Dmitriev, A., Quality function deployment and design risk analysis for the selection and improvement of fdm 3D printer. IOP Conference Series: Earth and Environmental Science. 2021. 666(6), 062123. doi: 10.1088/1755-1315/666/6/062123.

[2] Oskolkov, A., Bezukladnikov, I., and Trushnikov, D., Indirect temperature measurement in high frequency heating systems. Sensors. 2021; 21(7): 2561. doi: 10.3390/s21072561.

[3] Arias, G.G., Díaz, F.J., Ramirez, E.R., and Guzman, J.V., Thermal analysis by finite elements of hotends for 3d printing by fused filament fabrication. Periodica Polytechnica Mechanical Engineering. 2021; 65(2): pp. 129-133. doi: 10.3311/PPme.16203.

[4] Ramos, N., Mittermeier, C., and Kiendl, J., Experimental and numerical investigations on heat transfer in fused filament fabrication 3d-printed specimens. The International Journal of Advanced Manufacturing Technology. 2021. doi: 10.1007/s00170-021-07760-6.

[5] Ravoori, D., Lowery, C., Prajapati, H., and Jain, A., Experimental and theoretical investigation of heat transfer in platform bed during polymer extrusion based additive manufacturing. Polymer Testing. 2019; 73: pp. 439-446. doi: 10.1016/j.polymertesting.2018.11.025.

[6] Väisänen, A.J.K., Alonen, L., Ylönen, S., Lyijynen, I., and Hyttinen, M., The impact of thermal reprocessing of 3d printable polymers on their mechanical performance and airborne pollutant profiles. Journal of Polymer Research. 2021; 28(11): 432. doi: 10.1007/s10965-021-02723-7.

[7] Bits From Bytes, 3DTouch 3D Printer - Education Pack. Bits from Bytes Official Website, accessed 25 April 2025, available online: https://elco.crsndoo.com/bfb/www.bitsfrombytes.com:8080/usd/store/bfb-3dtouch-3d-printer-education-pack.

[8] Mileseey Tools, TR10 Thermal Imaging Camera with Affordable Price. Mileseey Tools, accessed 12 August 2025, available online: https://mileseeytools.com/products/tr10-thermal-imaging-camera-with-affordable-price.

[9] Pamasaria, H.A., Saputra, T.H., Hutama, A.S., and Budiyantoro, C., Optimasi keakuratan dimensi produk cetak 3d printing berbahan plastik pp daur ulang dengan menggunakan metode taguchi. JMPM (Jurnal Material dan Proses Manufaktur). 2020; 4(1). doi: 10.18196/jmpm.4148.

[10] Wicaksono, R.A., et al., Rancang bangun dan simulasi 3d printer model cartesian berbasis fused deposition modelling. Fadelandros & Sofyandi. 2021; 5(2): pp. 53-64.

[11] Edwards, T.J., Observations on the stability of thermistors. Review of Scientific Instruments. 1983; 54(5): pp. 613-617. doi: 10.1063/1.1137423.

[12] Prajapati, H., Ravoori, D., and Jain, A., Measurement and modeling of filament temperature distribution in the standoff gap between nozzle and bed in polymer-based additive manufacturing. Additive Manufacturing. 2018; 24: pp. 224-231. doi: 10.1016/j.addma.2018.09.030.

[13] Prajapati, H., Salvi, S.S., Ravoori, D., and Jain, A., Measurement of the in-plane temperature field on the build plate during polymer extrusion additive manufacturing using infrared thermometry. Polymer Testing. 2020; 92: 106866. doi: 10.1016/j.polymertesting.2020.106866.

[14] Zhang, J., Neeckx, J., Van Hooreweder, B., and Ferraris, E., Measurement, characterisation and influence of the air temperature above the build plate in fused filament fabrication. Additive Manufacturing Letters. 2021; 1: 100013. doi: 10.1016/j.addlet.2021.100013.

[15] Vanaei, H.R., Shirinbayan, M., Deligant, M., Khelladi, S., and Tcharkhtchi, A., In-process monitoring of temperature evolution during fused filament fabrication: a journey from numerical to experimental approaches. Thermo. 2021; 1(3): pp. 332-360. doi: 10.3390/thermo1030021.

[16] Zhang, J., Van Hooreweder, B., and Ferraris, E., T4F3: temperature for fused filament fabrication. Progress in Additive Manufacturing. 2022;7: pp. 971-991. doi: 10.1007/s40964-022-00271-0.

[17] Zhang, J., Wang, X., Yu, W., and Deng, Y., 2017, Numerical investigation of the influence of process conditions on the temperature variation in fused deposition modeling. Materials & Design. 2017; 130: pp. 59-68. doi: 10.1016/j.matdes.2017.05.040.

[18] Seppala, J.E., and Migler, K.D., Infrared thermography of welding zones produced by polymer extrusion additive manufacturing. Additive Manufacturing. 2016; 12: pp. 71-76. doi: 10.1016/j.addma.2016.06.007.